Energy Conversion and Management 151 (2017) 538–552

Contents lists available at ScienceDirect

Energy Conversion and Management

journal homepage: www.elsevier.com/locate/enconman

Thermoeconomic assessment of a solar polygeneration plant for electricity, water, cooling and heating in high direct normal irradiation conditions

Roberto Leiva-Illanes[a,b,*], Rodrigo Escobar[a], José M. Cardemil[c], Diego-César Alarcón-Padilla[d]

[a] Escuela de Ingeniería, Pontificia Universidad Católica de Chile, Vicuña Mackenna 4860, Santiago, Chile
[b] Departamento de Mecánica, Universidad Técnica Federico Santa María, Av. Federico Santa María 6090, Viña del Mar, Chile
[c] Departamento de Ingeniería Mecánica. Universidad de Chile, Av. Beauchef 851, Santiago, Chile
[d] CIEMAT-Plataforma Solar de Almería, Ctra. de Senés s/n, 04200 Tabernas, Almería, Spain

ARTICLE INFO

Keywords:
Solar energy
Concentrated solar power
Polygeneration
Thermoeconomic analysis
Multi-effect distillation
Absorption refrigeration

ABSTRACT

A thermoeconomic assessment of the joint production of electricity, fresh-water, cooling and heat for a solar polygeneration plant is carried out. The aims are to assess the actual cost of each product, to conduct a sensitivity analysis of investment, fuel cost and demand, and to evaluate the effects of solar field size and the sizing of thermal energy storage, for a polygeneration plant located in an area with high solar irradiation conditions and where there is demand for its production. The solar polygeneration plant is configured by a concentrated solar power (CSP) parabolic trough collector field with thermal energy storage and backup system, multi-effect distillation (MED) module, single-effect absorption refrigeration module, and process heat module. The solar polygeneration plant is simulated in a transient regime, in a representative location with high irradiation conditions, such as in northern Chile. Three configurations are investigated: two polygeneration schemes and one considering stand-alone systems. This study reveals that a solar polygeneration plant is more efficient and cost-effective than stand-alone plants for a zone with high irradiation conditions and proximity to consumption centers, such as mining industries, which require continuous operation and energy supply with fundamentally constant demand. Furthermore, according to northern Chilean market, solar polygeneration configurations are competitive regarding electricity, fresh-water, cooling and heat productions. Additionally, solar polygeneration plants can increase the economic profit by selling carbon credits and credits of renewable-energy quotas based on the Kyoto Protocol and Chilean legislation, respectively.

1. Introduction

Energy and fresh water are scarce in many places, especially in locations presenting high irradiation conditions, such as desert and arid zones, thus, the use of solar energy for producing energy and fresh water is an opportunity for economic development, energy security and climate change mitigation. Northern Chile, North-Africa and Australia are places with high irradiation conditions, availability of flat terrain, and with high consumption centers such as mining industries. Northern Chile is a good example for analysis, where its scarcity of energy and water, combined with the large mining facilities in the area, have pushed the demand for electricity, water, cooling and industrial process heat at competitive costs [1,2]. In fact, electricity, water and fuel prices have reached historical highs, negatively affecting the competitiveness of companies operating in the region. According to the Chilean Energy Ministry [3], in 2015, 17% and 34.4% of final energy consumption and electricity generated in the country respectively was consumed by the mining industry, while other industries account for 23% and 24.4% respectively. Chile has a geography that provides an extraordinary variety of climatic conditions and availability of water resources and solar energy. Chile extends 4 270 km from north to south. The north is mostly arid desert, the central zone having a more Mediterranean and the south being temperate and wet. The mining is mainly concentrate in the north regions where minerals are more abundant. The arid Atacama Desert in northern Chile contains great mineral wealth, principally copper. So, the energy consumption in northern Chile is mostly related to mining industries, which require continuous operation and energy supply with fundamentally constant demand. The main sources of energy supply for mining are electricity and fuels. The demand for electricity in 2015 was 18.7 TWh and 12.8 TWh in northern Chile and the cooper mining industry, respectively. At regional level, the electricity demand of the cooper mining industry was 11.0 TWh in Antofagasta

* Corresponding author at: Departamento de Mecánica, Universidad Técnica Federico Santa María, Av. Federico Santa María 6090, Viña del Mar, Chile, and Escuela de Ingeniería, Pontificia Universidad Católica de Chile, Vicuña Mackenna 4860, Santiago, Chile.
E-mail addresses: roberto.leiva@usm.cl, rleivaillanes@puc.cl (R. Leiva-Illanes).

http://dx.doi.org/10.1016/j.enconman.2017.09.002
Received 16 May 2017; Received in revised form 31 August 2017; Accepted 1 September 2017
Available online 14 September 2017
0196-8904/

Nomenclature

A	solar field aperture area, m^2
BS	backup fossil fuel energy system
capex	capital expenditure, USD
c_{ff}	fossil fuel cost, UD/(kWh)
$\dot{C}$	exergy cost rate, USD/h
$\dot{C}_{D,k}$	exergy destruction cost rate, USD/h
$\dot{C}_{F,k}$	exergy fuel cost rate, USD/h
$\dot{C}_{P,k}$	exergy product cost rate, USD/h
	unit exergy cost, USD/(kWh)
cfr	capital recovery factor, %
COP	Coefficient of performance, –
COCHILCO	Chilean Cooper Commission
CSP	concentrated solar power
DNI	direct normal irradiance, W/m^2
e	exergy specified, kJ/kg
$\dot{E}$	time rate of exergy or exergy rate, kJ/s
$\dot{E}_{sun}$	exergy rate from sun, kJ/s
$\dot{E}_D$	exergy destruction rate, kJ/s
$\dot{E}_{F,k}$	exergy fuel rate, kJ/s
$\dot{E}_{P,k}$	exergy product rate, kJ/s
$\dot{E}_{L,k}$	exergy loss rate, kJ/s
EPC	Engineering, Procurement, and Construction
FWP	feed water preheater
G	generator
HP	high pressure
i	discount rate, %
f_k	exergoeconomic factor, %
$LiBr/H_2O$	Lithium bromide/water
LP	low pressure
LCC	levelized cooling cost, USD/(kWh)
LEC	levelized electricity cost, USD/(kWh)
LHC	levelized process heat cost, USD/(kWh)
LWC	levelized water cost, USD/m^3
MED	multi-effect distillation
n	number of time periods, years
opex	operational expenditure or operation and maintenance cost, USD/a
P_{elect}	electricity selling price in the grid for industrial use, USD/(kWh)
PH	process heat plant
Poly	Polygeneration
$\dot{Q}$	heat rate, kJ/s
REF	Refrigeration plant
RO	reverse osmosis
r_k	relative cost difference, %
SAM	system advisor model software
SF	solar field
T_0	reference temperature, °C
TES	thermal energy storage
$\dot{W}$	work rate, kJ/s
$\dot{Z}$	non-exergy-related cost rate, USD/h
$\dot{Z}_k^{CI}$	capital investment cost rates, USD/h
$\dot{Z}_k^{OM}$	operating and maintenance cost rates, USD/h

Greek symbols

ψ	exergy efficiency
τ	average annual time of plant operation at nominal capacity

region [1]. Similarly, the demand for process heat and cooling in northern Chile is almost exclusively associated with mining activity. According to Chilean Cooper Commission (COCHILCO) [4], the demand for fuels in 2015 was 21.2 TWh in the copper mining industry, of these 16.7 TWh was used in ore transportation trucks, and 4.5 TWh in mining processes that requiring process heat such as smelting, refineries, leachable mineral treatments, and services. Of these processes, the leachable mineral treatments, and services require low temperatures, and its process heat demand was about 1.15 TWh. At the regional level, the fuel demand for copper mining industry was 12.1 TWh in Antofagasta region, and the demand of the leachable mineral treatments, and services was about 0.6 TWh. On the other hand, Chile in terms of water, agriculture accounts 77.8%, industry accounts for 9.1%, mining for 7.2% and drinking water for 5.9%. The proportions vary greatly between regions depending upon the climatic regions. The water consumption of the copper mining industry in 2015 was of 15.8 m^3/s, which is forecast to increase to around 21.5 m^3/s by 2026 due to the development of new projects and reduced ore concentration. At a regional level, the freshwater consumption of the copper mining industry in 2015 was of 5.7 m^3/s in Antofagasta region [1]. In contrast, Chile presents high availability of solar energy, especially in the northern region, which stands out as one of highest solar radiation rates worldwide. In this area, the annual average of daily global horizontal irradiation reaches levels higher than 8 kWh/m^2 and the daily average of direct normal irradiation presents values higher than 10 kWh/m^2 [5]. Hence, considering the large demand for electricity, fresh water and process heat, among other utilities, in northern Chile, and the high solar energy availability, we propose to analyze the potential for implementing polygeneration schemes, driven by solar energy.

A polygeneration scheme is an integrated process, which has three or more outputs that include energy flows, produced from one or more natural resources. Polygeneration systems can be classified as either topping, or bottoming cycle systems [6]. In a topping cycle, the priority is power production, i.e. the supplied fuel is first used to produce power and then thermal energy. It is the most popular and widely used method of polygeneration. In contrast, in a bottoming cycle, the priority is heat production, i.e. high temperature thermal energy is the primary product produced by the process and the heat rejected from the process is recovered to generate power. A polygeneration scheme has comparative advantages over individual stand-alone systems, since it allows for reduction in both the primary energy consumption and the emissions of greenhouse gasses by displacing fossil fuels. A polygeneration scheme allows for the integration of different technologies, maximizing the rational use of resources. Due to the complexity of dealing with several energy flows, the integration of such technologies could be evaluated through a thermoeconomic approach, which combines both economic and thermodynamic relations, aiming to reduce the total exergy cost rate of the products. That approach allows performing a complete assessment, considering the conversion efficiencies and economic benefits offered by the system [7].

1.1. Polygeneration technologies

Concentrated solar power (CSP) systems generate solar power by using mirrors to concentrate a large area of sunlight onto a small area. Electricity is generated when the concentrated light is converted to heat, which drives a power cycle that is usually a Rankine cycle. CSP technologies can be classified into four categories: CSP parabolic trough collector, central receiver (solar tower), linear Fresnel and dish-Stirling. Within the CSP technologies, CSP parabolic trough collector is considered as the most mature, accounting for 85% of the cumulative installed capacity; and presenting the lowest cost [8]. CSP parabolic trough collector allows for a simple integration of thermal energy storage (TES) and a backup system allowing to operate in periods of low

solar radiation, increasing its capacity factor. In this context, CSP systems with TES and backup system can provide full-load, steady state electricity generation, even on cloudy days or during the night, assuring predictable dispatchability to meet peak demands. All three basic conditions for the development of concentrated solar power plants are high levels of direct solar irradiance during most of the year, availability of flat terrain, and proximity to consumption centers. Regarding water desalination, polygeneration schemes commonly consider thermal driven technologies, such as multi-effect distillation (MED) and multi-stage flash or electric driven technologies, such as reverse osmosis (RO), which represent the most reliable and commercially proven technologies for desalination. Within the thermal technologies, MED is considered more attractive than multi-stage flash due to its lower energy consumption, low sensitivity to corrosion, low presence of scaling, and high development potential [9]. Furthermore, the possibility of operating MED plants at temperatures lower than 100 °C constitutes an interesting opportunity for coupling this technology to solar thermal systems [9]. Regarding the refrigeration process, absorption machines and vapor compression technologies are the most common systems employed for industrial cooling. Vapor compression systems are highly efficient refrigeration cycles that are currently dominating the market. However, it is not feasible to drive their operation using thermal energy. On the other hand, absorption refrigeration systems use thermal energy to drive a thermochemical cycle, demanding less than 1% of the electricity consumed by a vapor compression machine. Therefore, absorption refrigeration is more attractive than vapor compression refrigeration for a solar polygeneration scheme. The commercially available solutions for absorption refrigeration are mainly single and double effect cycles, where most of the absorption systems available on the market are single-effect systems [10].

The solar polygeneration plant proposed herein consists of a CSP parabolic trough collector with TES and backup system since it is the most developed and commercially-proven technology. In addition, a MED plant, a single-effect absorption refrigeration system, and a countercurrent heat exchanger as a process heat plant are considered because they are commercially available and allow for the use of thermal energy to drive the processes.

1.2. Integration scheme

Solar energy based heat and power systems is an attractive solution in order to satisfy the energy demands, such as electricity, process heat, hot water, heating, space cooling, refrigeration, and water. Within solar energy alternatives, the concentrated solar power technologies with parabolic trough collector, as a prime mover, allow for many integration alternatives in order to deliver several products. In this context, Modi et al. [11] presented a thorough review of solar energy based heat and power plants, considering only fully renewable plants with at least the production of electricity and heat/hot water for end use. They concluded that it is economically and environmentally beneficial to invest in both small and large capacity solar-biomass hybrid plants for combined heat and power production in the Nordic climatic conditions. Additionally, also suggest that the configuration with an organic Rankine cycle with solar thermal collectors and a biomass burner is particularly attractive for large capacity plants. Recently a new solar cogeneration plant named Aalborg CSP-Brønderslev CSP with Organic Rankine Cycle project [12] has been put into operation in Denmark for generating heat and power, a CSP system was integrated with a biomass-organic Rankine cycle plant. This is the first large-scale system in the world to demonstrate how CSP with an integrated energy system design can operate efficiently. However, currently there are no others solar polygeneration plants or solar cogeneration plants in operation that are coupled to a CSP plant. On the other hand, due to the huge potential of such schemes, the integration of CSP and desalination plants has been analyzed in several studies. Moser et al. [13] carried out a methodology for cost comparison, where different options for producing electricity (CSP, photovoltaic system, and wind power) and desalinated water (MED and RO) were analyzed and compared in terms of levelized electricity cost (LEC) and levelized water cost (LWC). The results for the LEC and LWC were 1.6% and 26.6% lower, respectively, in CSP-RO compared to CSP-MED. The same authors [14] developed a techno-economic model for the assessment of desalination plants (MED and RO), driven by conventional power plants, based on fossil fuels and renewable energies. The results showed that despite higher investment cost, LWC of CSP-Desalination was comparable to the cost of conventional desalination, where the variability of the results depend on the different operational and financial scenarios considered. Moreover, Fylaktos et al. [15] carried out an economic analysis of an electricity and desalinated water cogeneration plant in Cyprus. The results revealed that the CSP-Desalination concept is financially feasible for all systems, even though the electricity-only plant is economically more attractive. However, the findings also showed that LEC and LWC were 0.8% and 11.9% higher, respectively, for CSP-RO compared to CSP-MED. Recently, Palenzuela et al. [16] carried out a techno-economic analysis of different MED system schemes coupled to CSP plants and compared to the CSP-RO configuration. Results showed that replacing the condenser by low-temperature MED was mostly competitive in the Arabian Gulf, but CSP-RO performs better in the Mediterranean region, where evaporative cooling is employed. As described above, the results from different authors focused on techno-economic aspects using the first law of thermodynamics and economic relations for calculating the levelized costs (LEC and LWC); but not the second law of thermodynamics, as an exergy analysis. In this context, exergy is useful in identifying the causes, locations, and magnitudes of process inefficiencies. Moreover, several studies compared MED and RO technologies where the CSP-RO is considered to be better than CSP-MED in economic terms, but CSP-MED is driven by thermal energy and has low specific electricity consumption, high reliability, simple water pretreatment and low maintenance. Thus, MED is more attractive than RO for its integration into a polygeneration scheme.

Regarding the refrigeration process, solar absorption systems have been analyzed in several studies. In fact, Sarbu and Sebarchievici [10] reviewed a large number of studies about solar cooling, but the integration of power plants, specifically CSP plants, and absorption plants has been reported only in some studies in the literature [6,11]. Perdichizzi et al. [17] carried out an assessment of the integration of a CSP plant coupled to a double-effect steam driven absorption chiller. The results proved that absorption chillers fed by low-grade steam allowed to save a significant amount of electricity as compared with the use of compression chillers. Yet, in order to produce the same gross power in the cogeneration plant, the solar field requires a larger aperture area to deliver the heat demanded by the Rankine cycle.

Regarding the thermoeconomic analysis, the literature is extensive in polygeneration systems using fossil fuels as a main energy source, however, only a few studies have focused on thermoeconomic analyses of such systems driven by solar energy (CSP plants). Al-Sulaiman et al. [18,19] presented the formulation for the thermoeconomic optimization of three novel trigeneration systems based on Organic Rankine Cycle: Solid Oxide Fuel Cell -trigeneration, biomass-trigeneration, and solar-trigeneration systems. The solar-trigeneration system is made of a parabolic trough collector field including a two-tanks TES system coupled to an Organic Rankine Cycle; through a heat recovery system composed of a steam generator and a single-effect absorption chiller. The results revealed that the solar-trigeneration system offered the best thermoeconomic performance among the three configurations considered. Calise et al. [20] presented a novel solar polygeneration system, based on a hybrid system equipped with an Organic Rankine Cycle fuelled by a Parabolic Trough Collector solar field and by a geothermal well, a multi-effect distillation unit, and an absorption chiller. The results showed that the electricity price is a quite high, thus making the production scarcely competitive in the current energy market conditions; conversely, the price of the fresh water produced is

moderately competitive and it can be considered attractive in areas affected by the scarcity of water sources. Recently, Ortega et al. [21] performed a thermoeconomic analysis of the joint production of electricity and fresh water in a CSP plant, based on parabolic trough collector, MED and RO units. Four coupling schemes were investigated: a MED plant replacing the condenser of the CSP, a MED plant fed by one extraction of the turbine, RO driven directly from the electricity generated by the CSP plant and a RO plant connected to the local grid. Results showed that the best coupling option is the RO unit connected to the local grid, which obtained the lower LWC. However, between MED configurations, the results showed that the best coupling scenario was by replacing the condenser of the CSP plant with a MED system, in which case the LWC decreased by about 2.1%.

As described above, the integration and performance between CSP, MED, cooling and process heat plants has been analyzed extensively, focusing in cogeneration schemes. Some of those studies considered the levelized cost to evaluate the benefits of the integration, nevertheless, in schemes producing more products it is necessary to determine the relationship between the unitary costs of the different outputs [22]. Thermoeconomics allows to determine the cost of each product using cost allocation rules, allocating the resources consumed to the useful product of each component, and distributing its costs proportionally to the exergy flow. Hence, exergy is used as a basis for cost allocation of products. Few articles reported in the literature have applied thermoeconomic assessment to solar polygeneration systems, considering a concentrated solar power plant as primary driver. In that context, some important aspects have yet to be investigated, such as the different relationships between fuels and products, the effect of investment, fuel cost, and demand in the products costs; as well as the sizing of the solar field and the TES for these solar polygeneration systems considering high irradiation conditions. This solar polygeneration plant is very attractive in zones presenting high irradiation conditions, scarcity of water, availability of flat terrain, and proximity to consumption centers, such as the mining industries in the Northern Chile, Northern-Africa and Australia. Therefore, the objective of the present study is to apply a thermoeconomic assessment of CSP polygeneration plants, located in an area with high solar irradiation conditions and large demands for utilities, aiming to assess the actual cost of each product and conducting a sensitivity analysis regarding the most relevant parameters. The impact of integrating these different technologies is investigated based on the following parameters: total exergy cost rate of products and unit exergy costs. The results delivered provide useful information that could serve to decision-makers to point out the actual potential offered by solar polygeneration systems.

2. Methodology

The methodology considers the modeling of a solar polygeneration plant and the application of thermoeconomic evaluations. In brief, it is based in the following procedure: First, each stand-alone system is modeled and, afterward, each stand-alone model is validated against data reported in the literature. Then, according to technical restrictions, each technology is integrated composing a polygeneration plant. Three configurations are investigated: two polygeneration schemes and one configuration considering only stand-alone systems. The polygeneration plant is simulated considering an hourly resolution meteorological year [23], which represents the long-term behavior of the weather, in terms of a database of 8 760 hourly values. From the simulation, the plant's production is determined in hourly, monthly, and annual base, allowing to assess the contribution in each product from the sun, TES, and backup fossil fuel system. The solar thermal loop is composed of the solar field, the thermal energy storage, and the backup system. The modeling approach is based on a dynamic representation of the solar thermal loop and a steady state model of the power cycle, the desalination plant, the refrigeration plant, and the process heat unit. Those last operate in steady state conditions due to the energy provided by the solar thermal loop. Fig. 1 provides a flowchart of the overall simulation.

The software IPSEpro [24] was used for the simulations of each stand-alone plant and the solar polygeneration plants, both without TES/backup-system. IPSEpro software is composed of different modules; the main modules used in this research are IPSEpro-MDK, IPSEpro-PSE, and IPSEpro-PSXLink. IPSEpro-MDK (Model Development Kit) is a programming environment that offers all the capabilities required to define and build new component models and to translate them into a form that can be used by IPSEpro-PSE. IPSEpro-PSE (Process Simulation Environment) can establish mass and energy balances, simulating different kinds of processes, through iterative methods. These equation systems derived from the balances are solved by numerical methods (using the Newton–Raphson method) [24]. IPSEpro-PSXLink is an extension module that allows integrating IPSEpro-PSE projects with Microsoft Excel worksheets, which data exchange can be done in both directions: use data from Excel calculations as input for IPSEpro-PSE projects and use results of IPSEpro-PSE simulations in Excel spreadsheets for further post-processing with other software, such as in our case with MATLAB software. IPSEpro-PSE only develops steady state simulations, therefore, in order to analyze the dynamic behavior of the system, it is linked to a Microsoft Excel spreadsheet by IPSEpro-PSXLink where the input data, such as direct normal irradiance [23], the collector optical efficiency of solar field [25,26], and the demand for

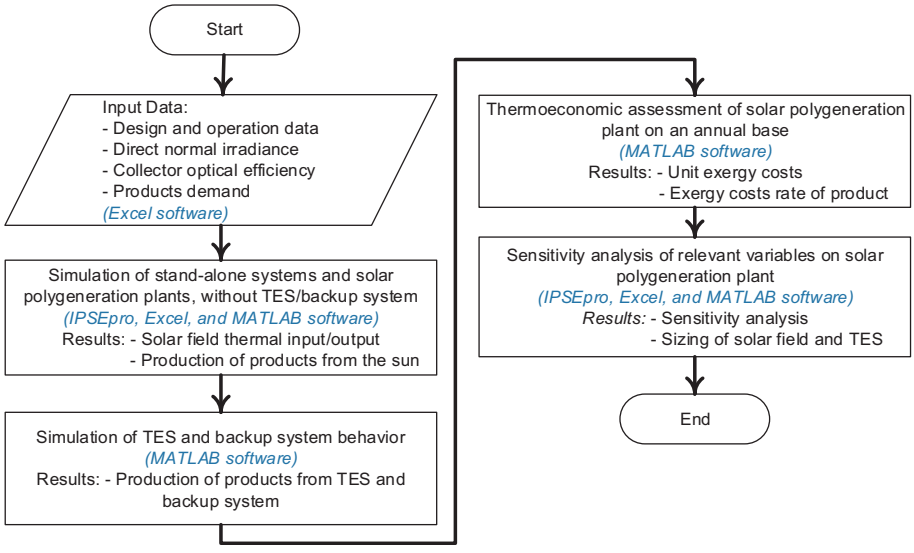

Fig. 1. Flowchart of the overall simulation.

products, are modified within each time-step. The results are the solar field thermal input/output, and the production of each product from the sun. After that, the simulation of the TES and backup system behavior was conducted using MATLAB software. The results are the production of each product from the TES and from the backup system; lastly, the total production of each product is the sum of production from the sun, TES, and backup system. This approach allows to simulate the polygeneration plant over a one-year period using an hourly time step.

Finally, the thermoeconomic model is solved on an annual base, for that purpose, an aggregation level is selected, allowing for the delimitation of boundaries for the analysis, and the physical and productive structures are determined, where fuel and product streams are established. Subsequently, different models are defined: thermodynamic, economic and thermoeconomic models [27]. The simulation of the thermoeconomic assessment was conducted using MATLAB software. The main parameters to analyze are total exergy cost rate of products and unit exergy costs. The total exergy cost rate of products is the amount of cost per unit time required to obtain the products, considering exergetic and non-exergetic parameters, by aggregating the exergy cost rate of fuel, the capital investment cost rates and the operating and maintenance cost rates. The unit exergy cost is the amount of cost per unit exergy required to generate each product.

The simulations considered the meteorological data from Crucero [23], in Antofagasta region, northern Chile (22.14 °S, 69.3 °W). Crucero is located at 1 146 meters above sea level and in extremely arid conditions. Moreover, it presents high irradiation levels: 3 389 kWh/(m^2 a) of direct normal irradiation and 2 571 kWh/(m^2 a) of global horizontal irradiation [5]. The analysis has been conducted for southern hemispherical conditions. Due to its high solar resource and its proximity to a transmission substation and different mining facilities, it is considered as one of the best sites for deploying solar energy technologies in Chile.

2.1. Design and modeling of a polygeneration plant

The first scheme analyzed herein is depicted in Fig. 2 and denominated as Poly 1, considering a CSP configuration that is analogous to the features of the Andasol-1 power plant, located in Granada (Spain) [25,26]. Based on these characteristics, the solar field is considered to be composed by parabolic trough collectors aligned on a north-south orientation, absorber tubes and organic compounds as heat transfer fluid. The collectors track the sun from east to west during the day. The design point date and time was defined as the 21st December solar noon for Crucero in Chile, where the thermal output of north-south oriented collectors is maximum at that date and time. The solar multiple is defined as a measure of the solar field aperture area as a function of the power block's nameplate capacity, the solar multiple assumed is equivalent to Andasol-1 at design point, which yields up to 510 120 m^2 of solar field aperture area as a stand-alone CSP plant. The power block consists of a regenerative Rankine cycle with reheat and six extractions, as suggested in Blanco-Marigorta et al. [28]. The TES is assumed as a two-tank indirect system using molten salts (60% $NaNO_3$, 40% KNO_3 by weight) as storage media. The full load hours of TES are the number of hours of thermal energy delivered at the power block's design thermal input level. This value is used for sizing the TES. The backup system supplies thermal energy directly to the heat transfer fluid used in the solar field, and the heat transfer fluid supplies thermal energy to the power block. The backup system permits to maintain the plant's power generation at design conditions when there is a lack of solar radiation and/or thermal energy from TES. The capacity factor is assumed as 96% [16] considering that in Chile there is no restriction on the consumption of fossil fuel in CSP plants. The fossil fuel used was natural gas. The main modification observed in Poly-1 regarding the configuration of Andasol-1 is the replacement of the condenser by a MED plant (between states 10 and 11). In addition, a refrigeration plant (REF) is coupled to the sixth turbine extraction (between states 9 and 43), and a process heat plant (PH) is coupled between feed water preheaters FWP3 and FWP4. Considering that the power output and solar multiple are fixed, the aperture area of the polygeneration system is increased by 20.9%, with respect to a stand-alone CSP plant.

In contrast, the configuration depicted in Fig. 3, denominated Poly 2, considers that the MED plant is coupled to the sixth turbine extraction (between states 9 and 11), the refrigeration plant is coupled to the fifth turbine extraction (between states 8 and 43) and the process heat

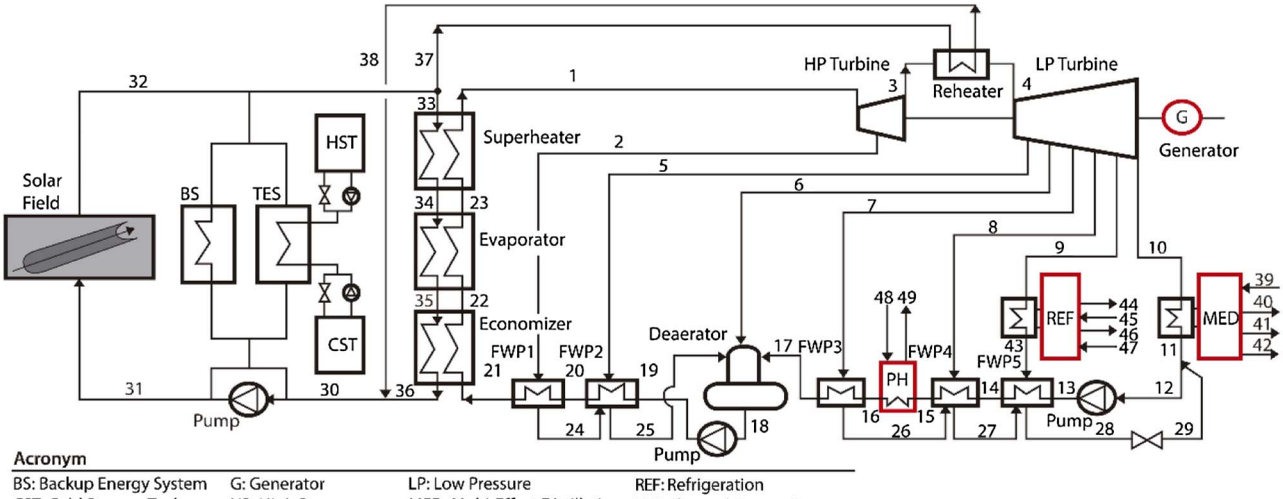

State	1	2	3	4	5	6	7	8	9	10	11	12	13	14	15	16	17	18	19	20	21	22	23	24	25
m kg/s	72.5	8.6	63.9	63.9	2.7	0.1	6.6	3.2	3.8	47.4	47.4	61.1	61.1	61.1	61.1	61.1	61.1	72.5	72.5	72.5	72.5	72.5	72.5	8.6	11.3
P bar	100.0	30.60	18.50	16.50	12.77	6.18	5.99	2.63	1.17	0.37	0.37	0.37	8.48	8.38	8.28	8.18	8.08	6.18	103.0	102.5	102.0	101.2	101.0	30.50	12.67
T °C	373.0	235.0	208.5	373.4	341.6	259.6	256.2	175.9	108.3	74.0	73.9	73.9	79.4	90.5	122.6	95.5	153.8	160.0	162.2	187.7	234.9	311.9	311.7	233.8	189.4

State	26	27	28	29	30	31	32	33	34	35	36	37	38	39	40	41	42	43	44	45	46	47	48	49
m kg/s	6.6	9.8	13.6	13.6	703.8	703.8	703.8	579.1	579.1	579.1	579.1	124.7	124.7	1588.1	430.2	555.6	602.3	3.8	281.8	297.5	297.5	281.8	61.8	61.8
P bar	5.89	2.53	0.97	0.37	8.90	12.30	11.90	11.80	11.80	11.70	11.90	11.90	8.90	1.00	1.00	1.00	1.00	1.07	1.00	1.00	1.00	1.00	1.00	1.00
T °C	157.1	126.8	97.8	73.9	292.7	293.0	393.0	379.3	379.3	313.7	292.7	393.0	292.7	25.0	52.8	35.0	39.5	101.5	35.0	10.0	6.0	25.0	63.0	90.0

Fig. 2. Polygeneration plant configuration. Poly 1. CSP + MED + REF + PH.

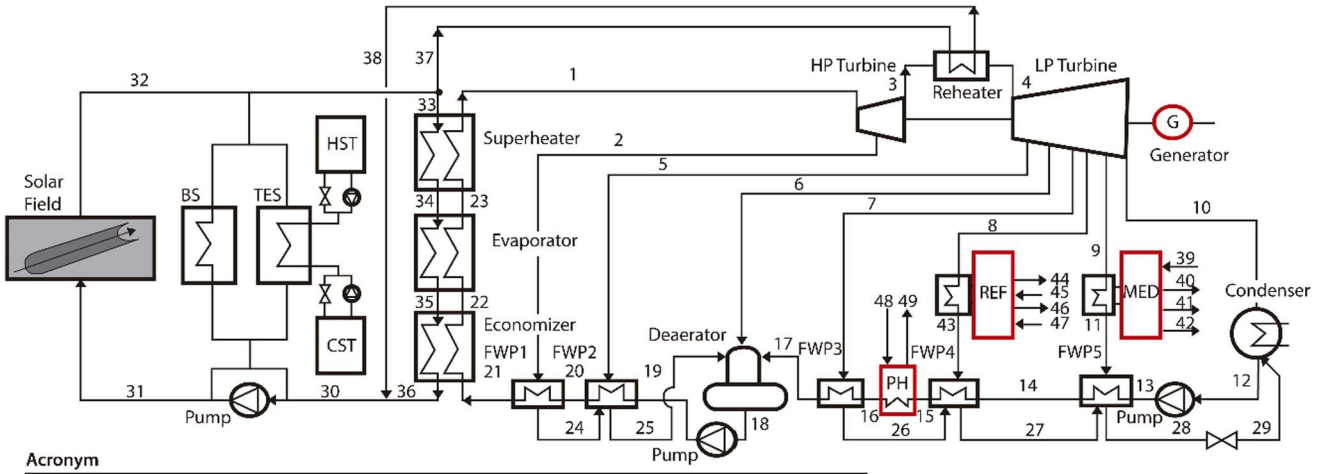

State	1	2	3	4	5	6	7	8	9	10	11	12	13	14	15	16	17	18	19	20	21	22	23	24	25
m kg/s	70.3	8.3	62.0	62.0	2.7	2.6	6.6	7.7	33.1	9.3	33.1	56.8	56.8	56.8	56.8	56.8	56.8	70.3	70.3	70.3	70.3	70.3	70.3	8.3	11.0
P bar	100.0	33.48	18.50	16.50	13.99	6.18	3.04	1.17	0.37	0.06	0.37	0.06	8.48	8.38	8.28	8.18	8.08	6.18	103.0	102.5	102.0	101.2	101.0	33.38	13.89
T °C	373.0	240.9	208.5	373.4	352.7	259.7	189.3	108.5	74.0	36.2	73.9	33.6	33.7	46.7	95.0	65.6	129.0	160.0	162.2	188.4	234.9	311.9	311.9	238.9	193.7

State	26	27	28	29	30	31	32	33	34	35	36	37	38	39	40	41	42	43	44	45	46	47	48	49
m kg/s	6.6	14.4	47.4	47.4	683.1	683.1	683.1	561.9	561.9	561.9	561.9	121.2	121.2	1107.6	300.0	387.6	420.0	7.7	281.8	297.5	297.5	281.8	61.8	61.8
P bar	2.94	0.97	0.27	0.27	8.90	12.30	11.90	11.90	11.80	11.70	11.60	11.90	8.90	1.00	1.00	1.00	1.00	1.07	1.00	1.00	1.00	1.00	1.00	1.00
T °C	131.8	97.8	65.6	65.6	292.7	293.0	393.0	393.0	397.3	313.7	292.7	393.0	292.7	25.0	52.8	35.0	39.5	101.5	35.0	10.0	6.0	25.0	63.0	90.0

Fig. 3. Polygeneration plant configuration. Poly 2. CSP + MED + REF + PH.

plant is coupled between feed water preheaters FWP3 and FWP4. For this configuration, the solar field aperture area is estimated as a 17.3% larger than a stand-alone CSP plant, which allows to ensure the power output level and to deliver the additional products.

The coupling point of each technology is selected according to the operating temperature constraints, imposed by each system and aiming to cause the minimum penalty in terms of power production. For instance, the MED plant must operate within a temperature range of 64 to 74 °C [9], while the desorber of the refrigeration plant should operate between 80 and 110 °C [10]. Because of that, in the Poly 1 scheme the turbine back pressure is modified from 0.06 to 0.37 bar. In this configuration is not possible to regulate the amount of fresh water produced, since the MED plant is driven by the heat rejected from the power cycle and consequently any problem in the MED plant will affect the electricity production. Hence, the production of fresh water is determined by the mass flow rate of the exhaust steam from at the outlet of the low-pressure turbine. However, the production from the refrigeration plant and the process heat plant can be regulated according to demand. On the other hand, in the Poly-2 scheme the LP turbine back pressure is the same as a stand-alone CSP plant. In this scheme, the MED, refrigeration and process heat plants are considered to be coupled to turbine extractions and feed-water, respectively, therefore, their outputs can be regulated according to the demand. Furthermore, in this configuration any problem on the operation of the MED plant does not affect the CSP plant, because the condensation of exhaust steam does not depend on the operation of the MED plant, however, the maximum fresh water production is limited to 385.9 kg/s, which corresponds to the case where all the turbine outlet steam is used as inlet steam in the MED plant. It should be mentioned that the output of water, cooling and process heat is dependent on the operating parameters of the rest of the plant. When it is reduced, for example, the production of process heat, the power cycle needs less input energy to generate at the nominal point (or other), and depending on the mode of operation, the control system could either reduce the energy input to power cycle by partial defocusing solar collectors, or reduce the thermal energy output from TES and/or backup system. Partial defocusing assumes that the tracking control system can adjust the collector angle in response to the capacity of the power cycle and thermal storage system.

In this study, the polygeneration plants were configured as a topping cycle, the priority is the production of electricity, and the other products are produced as a function of the thermal energy available in the power cycle. In Poly 1, the production of water is adjusted to the production of electricity. Poly 1 could run producing only electricity and water, but could not run producing the other products without producing electricity. On the other hand, Poly 2 could run producing only electricity, and in the same way, could not run producing the other products without producing electricity. Electricity and water are the priority in the mining industry.

Stand-alone configurations are also analyzed, aiming to validate the simulation models individually before integration, which also allow for comparing the performance of polygeneration plants with the same technologies, addressing the benefits of the integration. The simulation model of the CSP plant considers that the solar field outlet temperature is constant [29], and startup and shutdown procedures are not considered. Thus, the model of the power cycle of the stand-alone CSP plant was validated at the design point against the data of Andasol-1 reported by Blanco-Marigorta et al. [28]. The results show that the differences between the IPSEpro model and the reference are about 0.03% regarding the nominal steam mass flow rate and 0.28% regarding the gross power. Moreover, the stand-alone CSP plant was simulated with equivalent data of Andasol-1 configuration and was validated by comparing the results between the IPSEpro/Matlab model and those obtained from SAM software [26]. The results indicate differences of 3.6% in terms of annual net electricity, and 1.5% regarding the thermal efficiency.

The desalination plant is modeled considering 12 effects, parallel-cross feed MED plant and 11 feed preheaters, as suggested by Zak et al. [30]. In that context, the following assumptions are made in the thermodynamic modeling: vapors are salt free; the temperature difference between the condensation and evaporation are equal to the driving force for heat transfer in each effect; negligible heat losses to the surroundings; and the MED plant operates as a base load water station. The simulation model of the MED plant was validated considering the data reported by Zak et al. [30] and from El-Dessouky et al. [31]. The results

show no differences regarding total distillate water production, 5.46% error in terms of specific heat transfer area, and 7.81% regarding the Gained Output Ratio, which is defined as the mass of distillate produced for every mass unit of steam supplied to the desalination unit. Considering all the established assumptions and the large uncertainties involved in this analysis, relative errors lower than 9% are considered as having good accuracy, as stated in [32].

The refrigeration plant is defined as a single-effect LiBr-H_2O absorption chiller, and modeled as suggested by Herold et al. [33]. Regarding the thermodynamic modeling, the following assumptions are considered: LiBr solutions in the generator and the absorber are in equilibrium, the refrigerant outlets at the condenser and the evaporator are in a saturated state. Moreover, to avoid crystallization of the solution, the temperature of the solution entering the throttling valve should be at least 8 °C above crystallization temperature. The thermodynamic model of the refrigeration plant is validated against the data reported by Herold et al. [33]. The results show differences lower than 2.6% in terms of the cooling capacity and COP.

Finally, regarding the process heat plant, a countercurrent heat exchanger is configured to deliver the thermal load. Table 1 summarizes the main parameters of the CSP, MED, Refrigeration and Process Heat plants, according to the specifications above mentioned.

In this study, a constant demand for electricity, water, cooling and process heat was assumed, aiming to represent the large demands from the mining industry, which operates continuously and consequently presents a constant demand.

2.2. Thermoeconomic evaluations

The thermoeconomic evaluation was performed by selecting the proper aggregation level, allowing to delimitate the boundaries of the analysis, as depicted in Fig. 4. Then, physical and productive structures were defined, allowing to establish the fuels and products. After that, the thermodynamic, economic and thermoeconomic models [27] are applied according to the aggregation level.

2.2.1. Thermodynamic model

In order to perform thermodynamic modeling, mass, energy and exergy balances are applied, aiming to determine the exergy rate in each stream. The exergy balance is expressed as:

$$\sum_j \left(1-\frac{T_0}{T_j}\right)\dot{Q}_j - \dot{W} + \sum_{in} (\dot{m}_{in} e_{in}) - \sum_{out} (\dot{m}_{out} e_{out}) - \dot{E}_D = 0 \quad (1)$$

where $\dot{Q}$ is the heat power, T_0 is the temperature of reference, in K, $\dot{W}$ is exergy rate of work, $\dot{m}$ is the mass flow rate, e is the specific exergy, and $\dot{E}_D$ is the rate of exergy destruction. The subscripts j, in and out denote portion of boundaries, inlets, and outlets, respectively.

The exergy rate from solar radiation is evaluated using the Petela's equation [34], defined as follows,

$$\dot{E}_{sun} = A \cdot DNI \cdot \left(1 + \frac{1}{3}\left(\frac{T_0}{T_{sun}}\right)^4 - \frac{4}{3}\left(\frac{T_0}{T_{sun}}\right)\right) \quad (2)$$

where A is the solar field aperture area, DNI is the direct normal irradiance, and T_{sun} is the apparent temperature of the sun, assumed as 6 000 K [34].

The exergy analysis considered an environment temperature and pressure of 25 °C and 1.013 bar (1 atm), respectively. The reference mass fraction of LiBr and water salinity is considered 0.5542 and 0.042 (kg/kg), respectively. Finally, all the simulations assumed that the variations of kinetic energy and potential energy are negligible.

2.2.2. Economic model

The economic model was developed, aiming to determine the non-exergy-related cost rate $\dot{Z}_k$ for the k th component which is defined by aggregating the capital investment cost rate $\dot{Z}_k^{CI}$ and the operating and maintenance cost rate $\dot{Z}_k^{OM}$ (not included fuel cost such as fossil fuel or biomass, fuel cost is included into exergy-related cost rate), as follows

$$\dot{Z}_k = \dot{Z}_k^{CI} + \dot{Z}_k^{OM} = \frac{capex_k \cdot crf}{\tau} + \frac{opex_k}{\tau} \quad (3)$$

where τ is the annual average time of the plant's operation at nominal capacity, in hours/a; $capex$ is the capital expenditure, in USD; $opex$ is the operational expenditure, in USD/a; and crf is the capital recovery factor, defined as:

$$crf = \frac{i(1+i)^n}{(1+i)^n - 1} \quad (4)$$

where i is the discount rate and n is the number periods for the analysis. Considering the particular characteristics of the Chilean conditions, a

Table 1
Main parameters of polygeneration plants at design point.

Property	Value in Poly 1 and Poly 2	Unit
Thermal energy storage (TES)		
Type/storage fluid	2-tank/Molten salt	
Tank temperature (cold/hot)	292/386	°C
Annual storage efficiency	95	%
Full load hours of TES	12	h
Solar field		
Parabolic trough collector model	EuroTrough collector (Skal-ET)	
Absorber tube	Schott PTR-70	
Heat transfer fluid	Synthetic oil (DowTherm A)	
Collector optical efficiency	72.073	%
Irradiance at design day	1 010	W/m^2
Solar Field inlet temperature (inlet/outlet)	293/393	°C
Aperture area	Poly 1: 616 650/Poly 2: 598 510	m^2
Solar multiple	2.56	
Power conversion unit		
Gross power production	55.0	MW
HP turbine inlet pressure	Poly 1: 100.00/Poly 2: 100.00	bar
1^{st}/ 2^{nd}/ 3^{rd}/ 4^{th}/ 5^{th}/ 6^{th} extraction pressure	Poly 1: 30.6/12.77/6.18/5.99/2.63/1.17 Poly 2: 33.48/13.99/6.18/3.04/1.17/0.37	bar
LP turbine back pressure	Poly 1: 0.37/Poly 2: 0.06	bar
Isentropic efficiency (HP turbine/LP turbine)	85.2/85.0	%
Generator and motor efficiency	98.0	%
Pumps isentropic efficiency	70.0	%
MED		
Feed seawater intake temperature	25	°C
Feed seawater intake salinity	0.042	kg/kg
Feed seawater after down condenser temperature	35	°C
Maximum salinity in each effect	0.072	kg/kg
Top brine temperature	65	°C
Gained Output Ratio	9.07	kg/kg
Fresh water production	Poly 1: 37 168/Poly 2: 26 330	m^3/day
Concentration factor	1.7	–
Specific heat consumption	245.2	kJ/kg
Specific electricity consumption	1.5	kWh/m^3
Single stage absorption chiller		
Cooling capacity	5	MW_{th}
Chilled water temperature (inlet/outlet)	10/6	°C
Cooling water temperature (inlet /outlet)	25/35	°C
Inlet temperature desorber	108.49	°C
Coefficient of Performance (COP)	0.70	–
Process heat		
Process heat capacity	7	MW_{th}
Heat exchanger temperature (inlet/outlet) (state 48/state 49)	63/90	°C

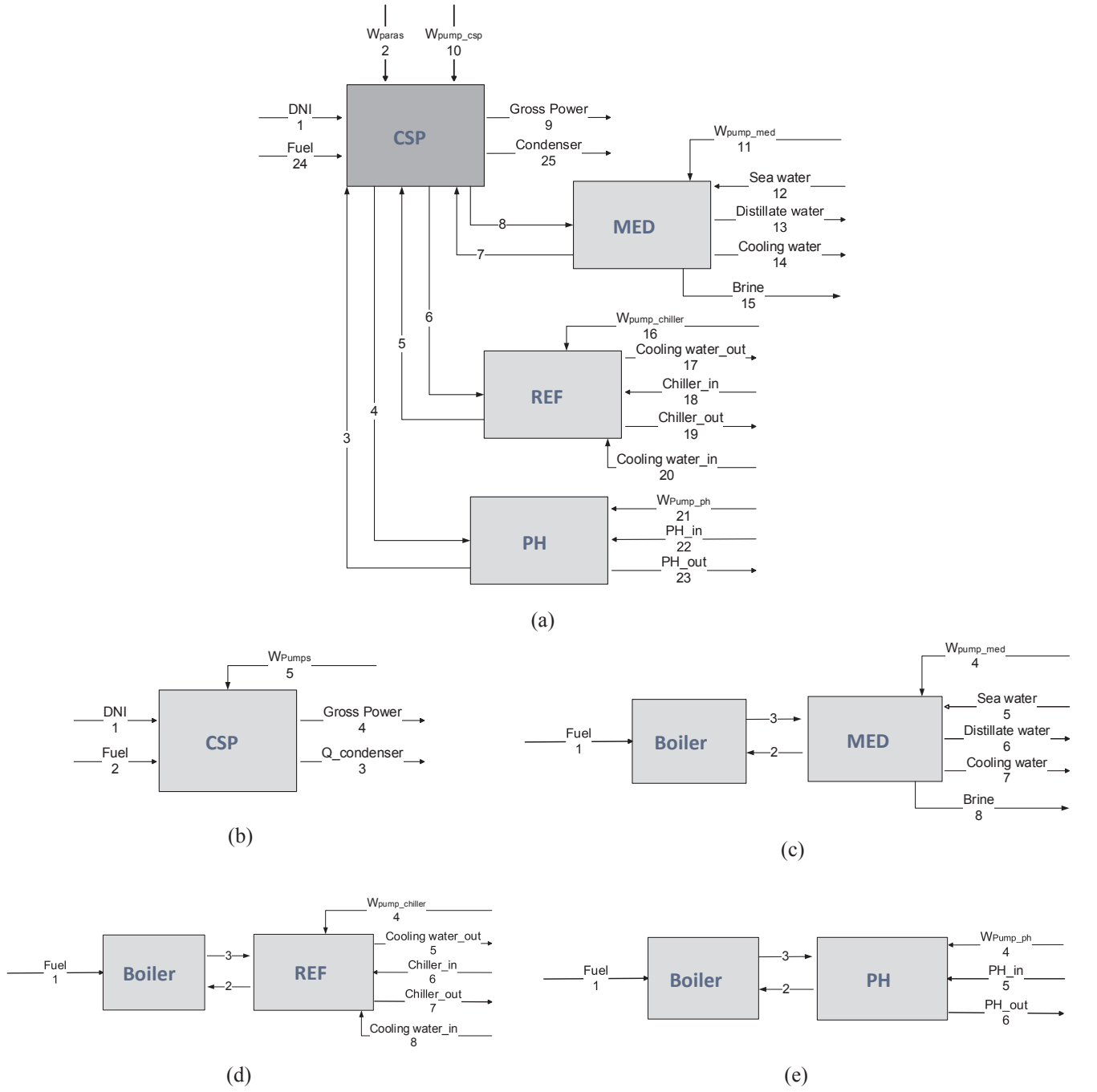

Fig. 4. Aggregation level for thermoeconomic assessment. (a) Polygeneration plant for Poly 1 and Poly 2 (Poly 1 does not have stream 25), (b) Stand-alone CSP, (c) Stand-alone MED, (d) Stand-alone refrigeration, (e) Stand-alone process heat.

horizon of 25 years and 10% discount rate were defined.

The economic considerations for the CSP parabolic trough collector plant are summarized in Table 2.

The main economic considerations for the MED plant are listed in Table 3, according to the specific costs reported in the literature. This table include the costs associated with the transportation of sea water to the plant location. The distance from the coast to the plant location is about 70 km and the altitude is about 1 146 m.

Finally, the refrigeration plant, process heat plant and boiler were modeled using unitary specific cost reported in the literature. Table 4 summarizes the information gathered for a refrigeration plant, and a process heat plant and the boiler.

2.2.3. Thermoeconomic model

The unit exergy cost and exergy cost rate $\dot{C}$ for each stream are calculated by economic balance, as follows

$$\sum_{in} (c_{in}\dot{E}_{in})_k + \dot{Z}_k = \sum_{out} (c_{out}\dot{E}_{out})_k \tag{5}$$

$$\dot{C} = c(\dot{m}e) \tag{6}$$

where, is the unit exergy cost, and $\dot{C}$ is the exergy cost rate. The subscript k denotes the k th component.

The exergy cost rate of product $\dot{C}_p$ is the sum of exergy cost rate of fuel $\dot{C}_f$ and non-exergy-related cost rate $\dot{Z}$. Hence, it considers exergetic and non-exergetic parameters.

For each subsystem, the fuel, product and auxiliary equations are

Table 2
Specific cost for CSP plant.

Cost	Value	Unit	Reference
Direct capital cost			
Site Improvements	28	USD/m^2	[26]
Solar Field	200	USD/m^2	[8]
Heat transfer fluid system	78	USD/m^2	[26]
Storage	35	USD/(kWh_{th})	[16]
Fossil Backup	60	USD/kW_e	[26]
Power Plant	850	USD/kW_e	[26]
Balance of plant	105	USD/kW_e	[26]
Contingency	7	%	[26]
EPC and Owner Cost	11	% of total direct capital cost	[26]
Total Land Costs	2	% of total direct capital cost	[26]
Sales of Tax applies of Direct Cost	4	% of total direct capital cost	[26]
Operational and Maintenance Costs			
Fixed Cost by Capacity	66	USD/(kW a)	[26]
Variable Cost by Generation	3	USD/(MWh)	[26]
Fossil Fuel Cost	0.0324	USD/(kWh)	[35]

Table 3
Specific cost for a MED plant.

Cost	Value	Unit	Reference
Direct capital cost MED			
Infrastructure and construction	1 500	USD/(m^3 day)	[36]
Contingencies (%)	10	%	[36]
Total	1 650	USD/(m^3 day)	
Operational and maintenance costs MED			
Chemical	0.025	USD/(m^3 a)	[36]
Maintenance	0.1	USD/(m^3 a)	[36]
Labor	2	% annualized total direct capital cost	[36]
Sea water transportation			
capex of piping	736	USD/m	[2]
capex of pumping	3.75	MUSD	[2]
Specific electricity consumption (pumping)	5	kWh/m^3	[2]

Table 4
Specific cost for a refrigeration plant, process heat plant and boiler.

Cost	Ref	PH	Boiler	Unit
Direct and Indirect Capital Cost	548.0	583.3	76.8	USD/kW_{th}
Operational and Maintenance costs	2	2	2	%
Reference	[37]	[38]	[38]	

defined in order to apply the economic balance for the polygeneration and stand-alone plants. In that context, the equations established for addressing that balance are summarized in Table 5, for the polygeneration schemes, and in Tables 6–9 for the stand-alone plants (CSP, MED, refrigeration, and process heat, respectively).

The exergy efficiency is defined as the ratio between the exergy rate of product and the exergy rate of fuel. Therefore, for the polygeneration schemes the exergy efficiency is determined by

$$\psi_{polygeneration} = \frac{\dot{E}_P}{\dot{E}_F} = \frac{\dot{E}_9 + \dot{E}_{13} + (\dot{E}_{19}-\dot{E}_{18}) + (\dot{E}_{23}-\dot{E}_{22})}{\dot{E}_1 + (\dot{E}_2 + \dot{E}_{10} + \dot{E}_{11} + \dot{E}_{16} + \dot{E}_{21}) + \dot{E}_{12} + \dot{E}_{24}} \tag{7}$$

and for stand-alone schemes, it is expressed as

$$\psi_{stand-alone} = \frac{\dot{E}_P}{\dot{E}_F} = \frac{\dot{E}_{4CSP} + \dot{E}_{6MED} + (\dot{E}_7-\dot{E}_6)_{Ref} + (\dot{E}_6-\dot{E}_5)_{PH}}{(\dot{E}_1 + \dot{E}_2 + \dot{E}_5)_{CSP} + (\dot{E}_1 + \dot{E}_4 + \dot{E}_5)_{MED} + (\dot{E}_1 + \dot{E}_4)_{Ref} + (\dot{E}_1 + \dot{E}_4)_{PH}} \tag{8}$$

To facilitate the thermoeconomic analysis, several assumptions were adopted along the simulation process, as listed below:

- The solar irradiance (stream 1) and the seawater intake (stream 12) have null costs.
- The unit exergy cost of fossil fuel (c_{ff}) is stated as 0.0324 USD/(kWh) [35].
- The unit exergy cost of electricity is equivalent for generator, pump and parasitic consumptions.
- The unit exergy costs related to the waste streams (14, 15, 17, and 20) are assumed as negligible.
- All products of the CSP plant present equivalent unit exergy cost, such as the thermal inputs for driving the MED, absorption chiller, process heat plant; and the output from the generator.
- The unit exergy cost in stand-alone plants (MED, refrigeration and process heat plants) is the electricity price from the grid for industrial use (P_{elect}), which is assumed to be 0.098 USD/(kWh) (Tariffs BT4 and AT4) [39].

The exergy destruction cost rate $\dot{C}_{D,k}$ in a component or process is a hidden cost, revealed only through a thermoeconomic analysis, as follows,

$$\dot{C}_{D,k} = c_{F,k}\dot{E}_{D,k} \tag{9}$$

where $\dot{C}_{D,k}$ is the exergy destruction cost rate of the k th component, $c_{F,k}$ is the unit exergy cost of fuel, and $\dot{E}_{D,k}$ is the rate of exergy destruction. Regarding the relative cost difference r_k, it expresses the relative increase in the average cost per unit exergy of the k th component, between fuel $c_{F,k}$, and product $c_{P,k}$, as follows,

Table 5
Economic balance in polygeneration plant. Poly 1 and Poly 2. Poly 1 does not have stream 25.

Subsystem	Fuel kW	Product kW	Economic balance USD/h	Auxiliary equations USD/(kWh)
CSP	$\dot{E}_1 + \dot{E}_2 + \dot{E}_{10} + \dot{E}_{24}$	$\dot{E}_9 + (\dot{E}_8-\dot{E}_7) + (\dot{E}_6-\dot{E}_5) + (\dot{E}_4-\dot{E}_3)$	$\dot{C}_9 + \dot{C}_8 + \dot{C}_6 + \dot{C}_4 + \dot{C}_{25} = \dot{C}_1 + \dot{C}_2 + \dot{C}_3 + \dot{C}_5 + \dot{C}_7 + \dot{C}_{10} + \dot{C}_{24} + \dot{Z}_{csp}$	$c_1 = 0$, $c_2 = c_9$, $c_3 = c_4$, $c_5 = c_6$, $c_4 = c_5$, $c_7 = c_8$, $c_7 = c_6$, $c_{10} = c_9$, $c_{24} = c_{ff}$, $c_{25} = 0$, $c_3 = c_9$
MED	$(\dot{E}_8-\dot{E}_7) + \dot{E}_{11} + \dot{E}_{12}$	$\dot{E}_{13}$	$\dot{C}_{13} + \dot{C}_{14} + \dot{C}_{15} + \dot{C}_7 = \dot{C}_8 + \dot{C}_{11} + \dot{C}_{12} + \dot{Z}_{med}$	$c_7 = c_8$, $c_{11} = c_9$, $c_{12} = 0$, $c_{14} = 0$, $c_{15} = 0$
Ref	$\dot{E}_{16} + (\dot{E}_6-\dot{E}_5)$	$\dot{E}_{19}-\dot{E}_{18}$	$\dot{C}_{17} + \dot{C}_{19} + \dot{C}_5 = \dot{C}_6 + \dot{C}_{16} + \dot{C}_{18} + \dot{C}_{20} + \dot{Z}_{ref}$	$c_5 = c_6$, $c_{16} = c_9$, $c_{17} = 0$, $c_{18} = c_{19}$, $c_{20} = 0$
PH	$\dot{E}_{21} + (\dot{E}_4-\dot{E}_3)$	$\dot{E}_{23}-\dot{E}_{22}$	$\dot{C}_3 + \dot{C}_{23} = \dot{C}_4 + \dot{C}_{21} + \dot{C}_{22} + \dot{Z}_{ph}$	$c_3 = c_4$, $c_{21} = c_9$, $c_{22} = c_{23}$

Table 6
Economic balance cost in stand-alone CSP plant.

Subsystem	Fuel kW	Product kW	Economic balance USD/h	Aux. equat. USD/(kWh)
CSP	$\dot{E}_1 + \dot{E}_2 + \dot{E}_5$	$\dot{E}_4$	$\dot{C}_3 + \dot{C}_4 = \dot{C}_1 + \dot{C}_2 + \dot{C}_5 + \dot{Z}_{csp}$	$c_1 = 0$, $c_2 = c_{ff}$, $c_3 = 0$, $c_5 = c_4$

Table 7
Economic balance cost in stand-alone MED plant.

Subsystem	Fuel kW	Product kW	Economic balance USD/h	Aux. equat. USD/(kWh)
Boiler	$\dot{E}_1$	$\dot{E}_3$–$\dot{E}_2$	$\dot{C}_3 = \dot{C}_1 + \dot{C}_2 + \dot{Z}_{boiler}$	$c_1 = c_{ff}$, $c_2 = c_3$
MED	$(\dot{E}_3$–$\dot{E}_2) + \dot{E}_4 + \dot{E}_5$	$\dot{E}_6$	$\dot{C}_2 + \dot{C}_6 + \dot{C}_7 + \dot{C}_8 = \dot{C}_3 + \dot{C}_4 + \dot{C}_5 + \dot{Z}_{med}$	$c_2 = c_3$, $c_4 = P_{elect}$, $c_5 = 0$, $c_7 = 0$, $c_8 = 0$

Table 8
Economic balance cost in stand-alone refrigeration plant.

Subsystem	Fuel, kW	Product, kW	Economic balance, USD/h	Aux. equat., USD/(kWh)
Boiler	$\dot{E}_1$	$\dot{E}_3$–$\dot{E}_2$	$\dot{C}_3 = \dot{C}_1 + \dot{C}_2 + \dot{Z}_{boiler}$	$c_1 = c_{ff}$, $c_2 = c_3$
Ref	$(\dot{E}_3$–$\dot{E}_2) + \dot{E}_4$	$\dot{E}_7$–$\dot{E}_6$	$\dot{C}_2 + \dot{C}_5 + \dot{C}_7 = \dot{C}_3 + \dot{C}_4 + \dot{C}_6 + \dot{C}_8 + \dot{Z}_{ref}$	$c_2 = c_3$, $c_4 = P_{elect}$, $c_5 = 0$, $c_6 = c_7$, $c_8 = 0$

Table 9
Economic balance cost in stand-alone process heat plant.

Subsystem	Fuel kW	Product kW	Economic balance USD/h	Aux. equat. USD/(kWh)
Boiler	$\dot{E}_1$	$\dot{E}_3$–$\dot{E}_2$	$\dot{C}_3 = \dot{C}_1 + \dot{C}_2 + \dot{Z}_{boiler}$	$c_1 = c_{ff}$, $c_2 = c_3$
PH	$(\dot{E}_3$–$\dot{E}_2) + \dot{E}_4$	$\dot{E}_6$–$\dot{E}_5$	$\dot{C}_2 + \dot{C}_6 = \dot{C}_3 + \dot{C}_4 + \dot{C}_5 + \dot{Z}_{ph}$	$c_2 = c_3$, $c_4 = P_{elect}$, $c_5 = c_6$

$$r_k = \frac{c_{P,k} - c_{F,k}}{c_{F,k}} \tag{10}$$

Finally, the exergoeconomic factor [27] is expressed as the ratio between the contribution of the non-exergy-related costs and the exergy related costs (cost of exergy destruction and exergy losses).

$$f_k = \frac{\dot{Z}_k}{\dot{Z}_k + c_{F,k}(\dot{E}_{D,k} + \dot{E}_{L,k})} \tag{11}$$

As described above, this methodology allows to assess the exergy cost rate, unit exergy cost for each product and the exergoeconomic factors in order to compare the performance of polygeneration schemes and stand-alone plants with the same capacity configuration. If the capacity configuration is different, as the case of Poly 1 and Poly 2 that have different capacities of MED plant, it is only possible to compare the unit exergy cost for each product, but not the exergy cost rate.

3. Results and discussion

3.1. Production and thermoeconomic assessment in base cases

Fig. 5a depicts the daily average of monthly productions of electricity, desalinated water, cooling and process heat of the Poly 1 scheme from the solar (considering from the sun and TES, and without backup system). The behavior of the plant shows seasonal variation, presenting lower production during the winter (June and July) and in summer almost all the energy comes from the sun. In contrast, in February, the productions decreased because there are episodes of persistent cloud cover resulting from moisture by the Altiplanic Winter. Fig. 5b presents the relative energy consumption from the solar and from the backup system, where the annual solar contribution is 71.6%. The same tendency is observed in Poly 1 and Poly 2 schemes.

The annual production of electricity, desalinated water, cooling and process heat, and exergy efficiencies of base cases are presented in

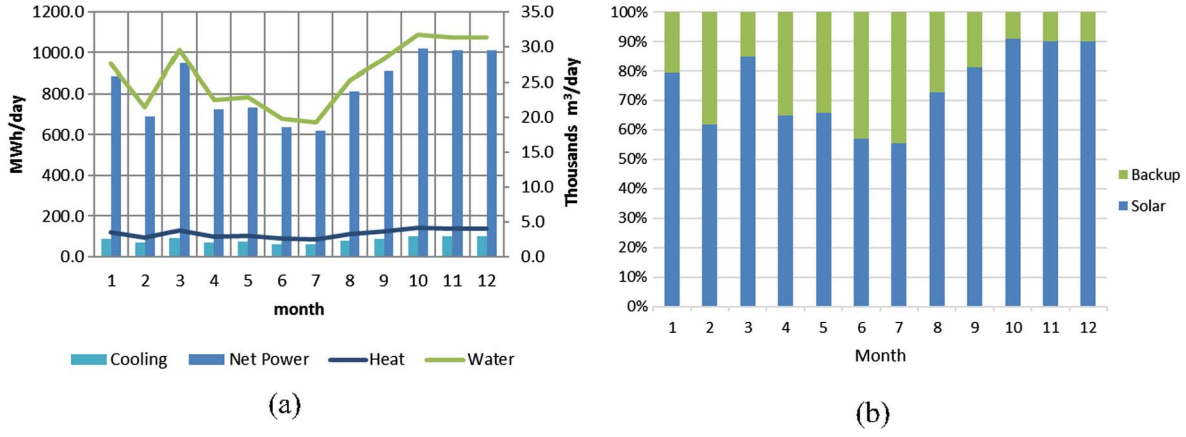

Fig. 5. (a) Monthly productions from the solar. (b) Monthly percentage production from the solar and from the backup.

Table 10
Annual productions and exergy efficiencies in base cases.

Item	Poly 1	Poly 2	Stand-alone
Gross power, GWh/a	463.1	463.1	463.1
Net power, GWh/a	408.5	415.3	449.8
Fresh water, Mm^3/a	13.2	9.2	13.2
Cooling, GWh/a	42.0	42.0	42.0
Heat, GWh/a	58.9	58.9	58.9
Exergy efficiency, %	27.1	27.6	18.7

Table 10. The net power is the electric energy provided by the generator minus the parasitic loads of the plant. Fresh water production in Poly 1 is about 40% higher than Poly 2, because the power block condenser was replaced by a MED plant in the Poly 1 scheme, and the MED plant was driven by all the heat rejected from the power cycle. Stand-alone MED plant produces the same amount of fresh water as Poly 1 in order to compare them. Regarding exergy efficiencies, they were calculated by Eqs. (7) and (8) for polygeneration and stand-alone schemes respectively. Poly 2 is more efficient than Poly 1, and polygeneration is more efficient than stand-alone plants. Exergy efficiency provides a measure of how closely the operation of a system approaches the ideal, or theoretical upper limit. Exergy efficiency gives information of process performance because they weigh energy flows according to their exergy contents and they separate inefficiencies into those associated with effluent losses and those due to irreversibilities [7].

Exergy cost rate of products and unit exergy costs of both polygeneration schemes are presented in Table 11. It should be mentioned that the unit exergy cost of water associated with the sea water transportation cost was included in this cost and it was calculated considering the $capex_{piping}$, the $capex_{pumping}$, the specific electric consumption, the annual water production and the electricity price from the grid for industrial use (P_{elect}).

In Poly 1 and Poly 2 configurations, the unit exergy costs are lower than stand-alone systems, thus, polygeneration schemes are better than stand-alone systems. On the other hand, Poly 1 produces electricity, fresh water and cooling at a lower unit exergy cost than Poly 2. Therefore, Poly 1 is the best alternative, considering that the unit exergy cost is calculated from economic balance, which the total exergy cost rate of products includes the exergy cost rate of fuel, the capital investment cost rates and the operating and maintenance cost rates.

Comparing the costs observed in the Chilean market, at the proximities of Crucero, the price of electricity tender is 0.1148 USD/(kWh) [40] for Cerro Dominador Solar Thermal Plant (CSP plant) in northern Chile. The unit exergy cost of electricity in Poly 1 and Poly 2 are lower than this price of electricity tender. Concerning water, the fresh water price in northern Chile is between 2.1 and 5.6 USD/m^3 [2,41]. The main factors in the price of water is the electricity cost and the delivery point. Moreover, the cooling price is 0.0392 USD/(kWh), considering an electricity price of 0.098 USD/(kWh) [39] (Tariffs BT4 and AT4) and a COP for a vapor compression chiller of 2.5. Finally, the process heat price is 0.036 USD/(kWh), considering a natural gas cost of 0.0324 USD/(kWh) [35] and a boiler efficiency of 90% [26]. Hence, according to the Chilean market, solar polygeneration plants are competitive in terms of electricity, fresh water, cooling and heat productions.

Additionally, solar polygeneration plants can increase the economic profit by selling carbon credits (certified emission reductions) according to the clean development mechanism of the Kyoto Protocol, and/or selling credits conforming with the renewable energy quota established by Chilean legislation [42]. The emission factor of Northern Chile Interconnected System grid is 0.764 $tonCO_2eq/(MWh)$, thus, by electric production it is possible to reduce the emissions by 312 078 $tonCO_2eq/a$ in Poly 1. Considering a carbon price of 0.39 $USD/tonCO_2eq$ [43], carbon credits could represent an income of 0.12 MUSD/a. With regards to the renewable energy quota, the price of renewable energy credits is assumed as 27.4 USD/(MWh), which is the fine for non-compliance of the renewables energy quota, thus, by electric production it is possible to increase the income by 11.19 MUSD/a, which would reduce the unit exergy cost of electricity by 0.2% and 18.3%, respectively.

In conformity with thermoeconomic indicators summarized in Table 12, the sum $\dot{C}_D$ plus $\dot{Z}$ shows the improvement potential in order to raise cost effectiveness. Components with a high cost rate ($\dot{C}_D$ plus $\dot{Z}$) and high relative cost difference, such as CSP, are significant for further comparison analysis. Moreover, the exergoeconomic factor is used to identify the major cost source, both capital investment and exergy destruction cost. CSP has a high exergoeconomic factor, the rule says that if the exergoeconomic factor is high, it is suggested to evaluate whether it is cost effective to reduce the capital investment for the component at the expense of the component efficiency, in other words, the system performance may be improved by decreasing the investment cost of the CSP plant. Conversely, if the exergoeconomic factor is low, such as MED, cooling and heat plants, it is suggested to evaluate whether the component efficiency (and the investment cost) should be increased, in this case the associated cost of thermodynamic inefficiencies is more significant than the investment costs for the component under consideration. Hence, according to those criterions, the CSP plants may be improved and the other plants are not a priority for improvement. It is recommended to reduce the non-exergy-related cost rate at the expense of its efficiency at the CSP plant. It should be noted that, in general, when a plant is less efficient its investment cost is lower.

3.2. Sensitivity analysis of investment cost, fuel cost and demand

A sensitivity analysis of investment cost of TES, solar field (SF), MED plant, refrigeration plant and process heat plant was carried out. Fig. 6 depicts the effect over total exergy cost rate of products for Poly 1 and Poly 2. The results show that the most significant changes in the total exergy cost rate of products was due to the variation of the investment costs of solar field, TES and MED. The changes are marginal in the case of refrigeration plant and process heat plant, because the investment costs of refrigeration plant and process heat plant were significantly lower with respect to the investment cost of a CSP plant.

To illustrate the effect of investment cost over unit exergy costs, comparative graphs are presented in Fig. 7 for Poly 1. The same tendency is observed in both configurations of polygeneration plants. According to the results, variation of investment costs of solar field and TES affects each unit exergy cost of electricity, fresh water, cooling, and heat, respectively. In contrast, variation of investment cost of MED, refrigeration plant and process heat plant affect only the unit exergy cost associated with the product that each one produces; for example, variation of investment cost of MED only influences the unit exergy cost of water, the variation of investment cost of refrigeration plant only influences the unit exergy cost of cooling, and the variation of investment cost of process heat plant only influences the unit exergy cost of heat. This behavior is due to the unit exergy costs in the streams that connect the CSP plant with MED, refrigeration plant and process heat plant have the same value, as indicated in Table 5. According to the thermoeconomic, if a process has more than one product, the irreversibilities of the process are distributed proportionally to the exergy of

Table 11
Exergy cost rate of products and unit exergy costs.

Item	Poly 1	Poly 2	Stand-alone
$\dot{C}_{p,total}$, USD/h	10 507.4	9 769.4	13 630.0
$c_{p\ electricity}$, USD/(kWh)	0.1058	0.1114	0.122
$c_{p\ water}$, USD/m^3	2.746	3.008	4.0355
$c_{p\ cooling}$, USD/(kWh)	0.036	0.038	0.055
$c_{p\ heat}$, USD/(kWh)	0.024	0.018	0.038

Table 12
Thermoeconomic indicators in polygeneration schemes.

Plant	$\dot{C}_{D,k} + \dot{Z}_k$ USD/h		r_k%		f_k%	
	Poly 1	Poly 2	Poly 1	Poly 2	Poly 1	Poly 2
CSP	7 048.2	6 944.4	91.3	91.6	81.6	81.1
MED	4 085.9	3 127.5	94.6	94.8	61.0	62.5
Cooling	163.6	175.8	83.1	83.4	22.4	20.8
Process heat	57.3	11.0	34.5	8.8	6.6	34.2

the output flows, and then the unit costs of all products are equal. On the other hand, according to the cost formation process, the unit exergy cost of water, cooling and heat are functions of the unit exergy cost of electricity, their own investment cost and exergy rates. And the unit exergy cost of electricity is function of fuel cost, exergy rates and the investment cost of CSP plant.

A sensitivity analysis of fossil fuel cost, and demands of cooling, heat and fresh water was also carried out, which are depicted in Fig. 8. Fig.8a shows that variation in the fuel cost impact each unit exergy cost, but is more significant in the unit exergy costs of electricity, heat and water. Regarding the demand variations shown in Fig.8b–d, the unit exergy cost of product (cooling, heat or water) is increased as the demand of this product is reduced, because the installed capacity is underused and the investment cost is charged to a low product production.

3.3. Effects of sizing solar multiple and TES

An important aspect in the CSP plant is the solar field size (solar multiple) and the amount of thermal energy storage. In this context, Fig. 9 shows the total exergy cost rate of products as a function of the solar multiple and the storage capacities for Poly 1 and Poly 2 schemes. According to the results, the minimum total exergy cost rate of product is attained with a solar multiple of 1.4 and 1.8, and TES of 3 and 6 h in Poly 1 and Poly 2, respectively. The values are 10 222 USD/h and 9 523 USD/h, respectively. There is a difference of 2.3% and 2.1% between the optimal configuration and base cases for Poly 1 and Poly 2, respectively. However, there is a relatively small difference between other configurations, such as, a plant with a solar multiple of 2.2 and 9 h of TES, or with a solar multiple of 1.8 and 6 h of TES. This behavior is due the total exergy cost rate is dominated by the sizing of solar field and TES, hybridization (backup system) levels, and the location of the plant (level of direct normal irradiation). The last point was not sensitized in this study. An optimal solar field area should maximize the time in a year that the field generates enough thermal energy to drive the power cycle at its rated capacity, minimize *capex* and *opex*, and use TES and backup system efficiently and cost effectively. The problem of choosing an optimal sizing of solar field and TES involves analyzing the trade-off between a larger solar field and TES in order to maximize the system's output (electricity, water, cooling and process heat) and project revenue, and a smaller solar field and TES that minimizes *capex* and *opex*.

The optimal point is very sensitive to the investment costs of solar field and TES, as well as to the fossil fuel cost. The decision about the size of solar field (solar multiple), levels of TES and backup system to develop will depend on the additional costs of their expansion, relative to the additional production to dispatch. On the other hand, without backup system, the minimum total exergy cost rate of product is attained with a solar multiple of 2.8 and TES of 15 h in both polygeneration schemes.

Concerning unit exergy cost, in Fig. 10 the minimum unit exergy cost is presented for Poly 1: 0.1022 USD/(kWh), 2.705 USD/m^3, 0.035 USD/(kWh) and 0.023 USD/(kWh) for electricity, water, cooling and heat, respectively. The concept of unit exergy cost is analogous to levelized cost, where the main difference is that unit exergy cost is the amount of cost per unit exergy required to produce each product. Unit exergy cost includes exergy costs and non-exergy costs (costs of installing and operating), while the levelized cost is the amount of cost per unit energy required to produce each product. It includes only non-exergy costs (cost of installing and operating).

In a CSP plant, the criterion for selecting the optimal size of the plant is the minimum LEC [25,29]. However, in the case of solar polygeneration plants, the criterion should be the minimum total exergy cost rate of products $\dot{C}_p$, as the thermoeconomic method allows to charge the costs according to the type and amount of each utility employed for generating such a product, where the exergy is used for allocating the costs, and the total exergy cost rate of products includes the exergy cost rate of fuels and non-exergy-related cost rate. Additionally, exergy cost rate of products allows to aggregate different kinds of products, such as, electricity, fresh water, cooling and process heat. On the other hand, conventional economic analysis does not provide criteria for apportioning the carrying charges, fuel costs, and *opex* to the various products generated in the same system [27] and it is based only on the first law of thermodynamics, which states the principle of conservation of energy.

4. Conclusions

A solar polygeneration scheme is proposed as an alternative for the supply of electricity, fresh water, cooling and heat for a zone with high irradiation conditions, scarcity of water, availability of flat terrain, and a short distance to consumption centers, such as those in northern Chile. For that reason, a thermoeconomic assessment of a solar polygeneration plant using a CSP parabolic trough collector of 50 MW with TES and backup system, a multi-effect distillation MED plant, a single-effect absorption refrigeration plant, and a countercurrent heat exchanger for process heat was carried out. Three configurations were investigated: two polygeneration schemes and one configuration

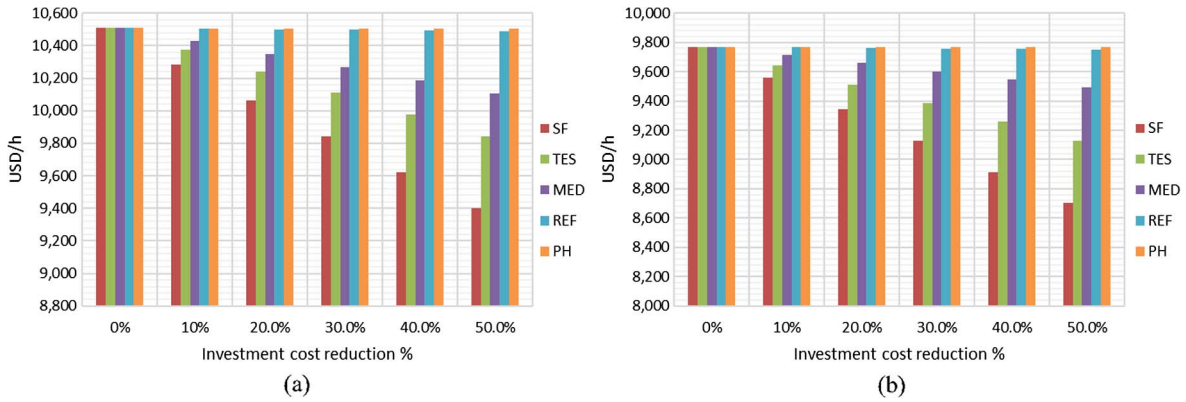

Fig. 6. Sensitivity analysis of investment cost. Effect in total exergy cost rate of products. (a) Poly1. (b) Poly 2.

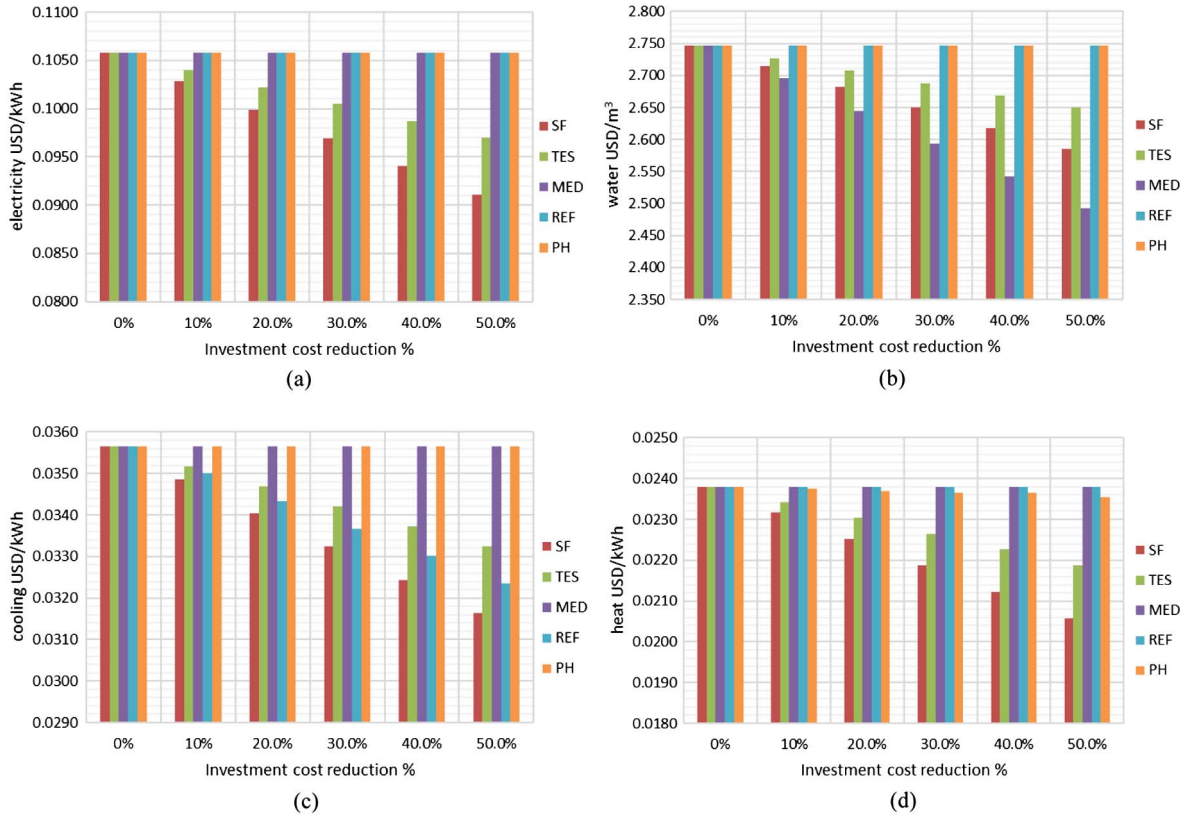

Fig. 7. Sensitivity analysis of investment cost in Poly 1. Effect in unit exergy cost of: (a) electricity, (b) water, (c) cooling, (d) heat.

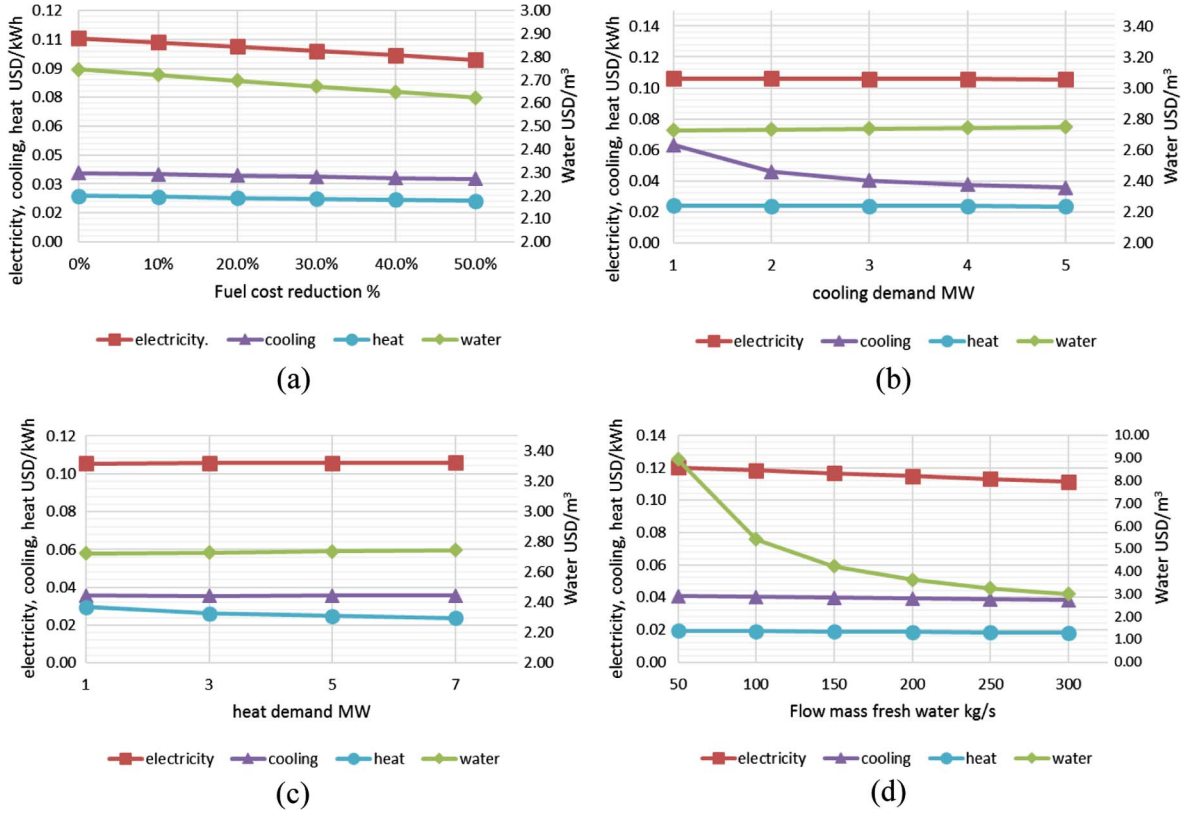

Fig. 8. Sensitivity analysis of: (a) fuel cost, (b) cooling demand, (c) heat demand, (d) fresh water demand.

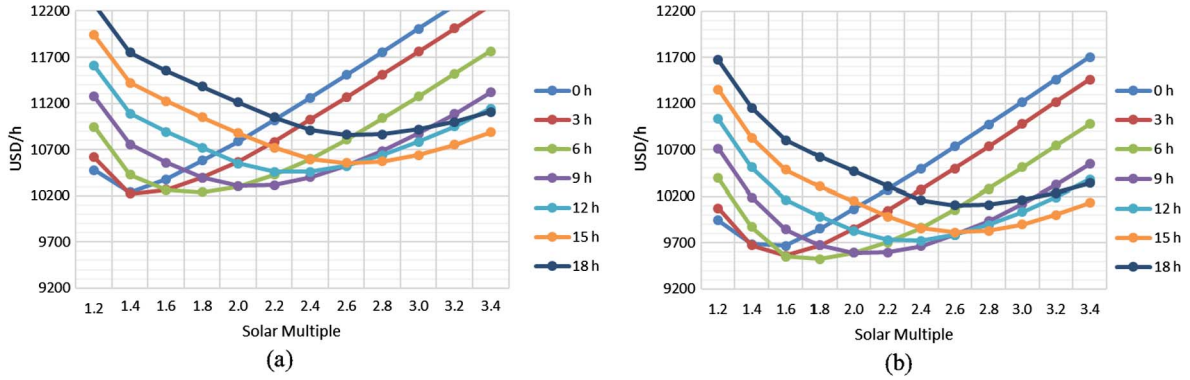

Fig. 9. Total exergy cost rate of products as a function of the solar multiple and the hours (h) of TES. (a) Poly 1. (b) Poly 2.

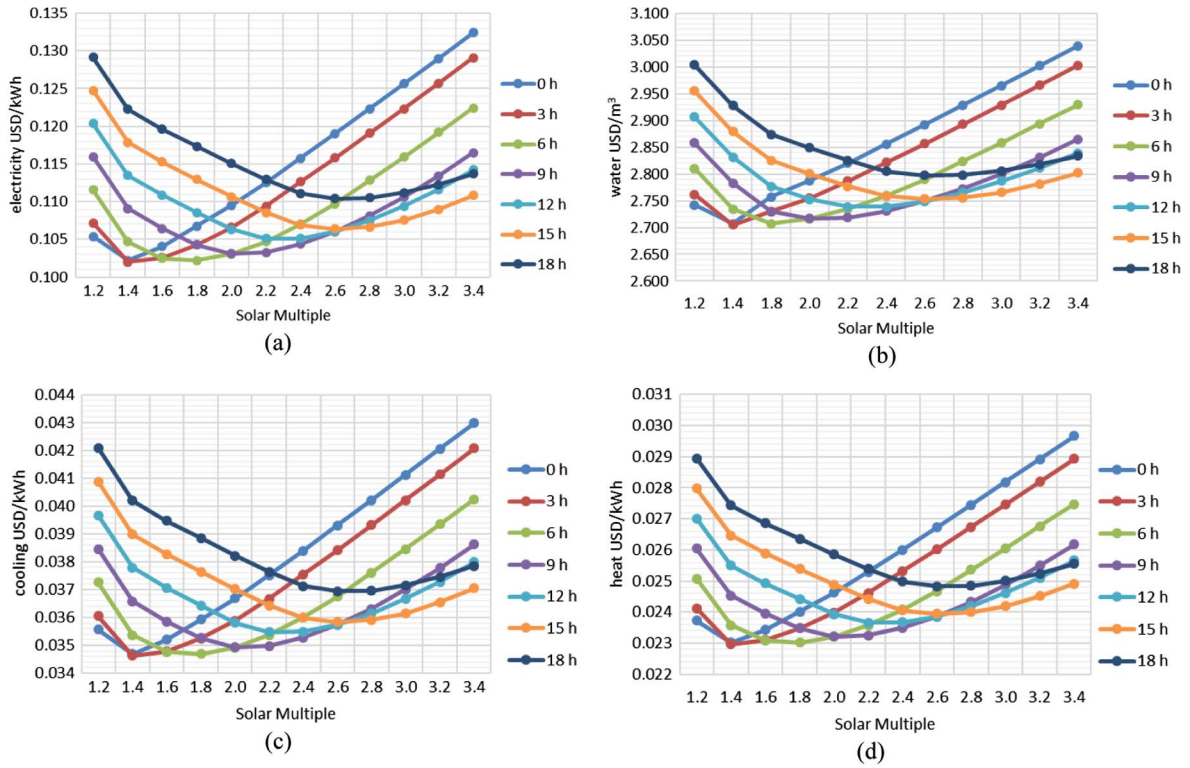

Fig. 10. Unit exergy cost for Poly 1 configuration (a) electricity, (b) water, (c) cooling, (d) heat.

considering only stand-alone systems for comparison purposes.

The results show that, in terms of total exergy cost rate of products, unit exergy cost, and exergy efficiency, the solar polygeneration schemes are more economically attractive than stand-alone systems with high irradiation conditions and proximity to consumption centers. Therefore, a solar polygeneration plant is a cost-effective system making a more efficient use of the available resources.

According to the results, the recommended configuration for a solar polygeneration plant is the one where the MED plant has replaced the condenser of the CSP plant, the refrigeration plant is coupled in the sixth turbine extraction, and the process heat plant is coupled between feed water preheaters. This plant was the most cost-effective configuration.

In conformity with North Chilean market, the solar polygeneration plants are competitive. Moreover, solar polygeneration plants can increase the economic profit with the sale of carbon credits according to the Kyoto Protocol and the sale of credits, conforming with the renewable energy quota established by Chilean legislation.

The sensitivity analysis of investment cost show that the investment costs of solar field and TES are more influential on the total exergy cost rate and unit exergy cost of the plant. Therefore, the key areas where cost reductions need to be achieved are the solar field and TES.

The traditional criterion for selecting the optimal size of a CSP plant is the minimum LEC but in the case of solar polygeneration plants, the criterion should be the minimum total exergy cost rate of products $\dot{C}_p$, as the thermoeconomic method uses exergy as a criterion to allocate costs and allows to perform an assessment considering the conversion efficiencies and economic benefits offered by the system.

In future studies, a comparison of the thermoeconomic and the levelized cost methods in a solar polygeneration plant should be conducted to determine and compare the different unit costs of each product, such as, unit exergy costs (electricity, water, cooling and heat) and levelized costs (LEC, LWC, LCC and LHC). As another prospective action, a thermoeconomic assessment with a low aggregation level in CSP plant should be done by individual components, such as turbines, preheaters, solar field, among others, in order to understand which specific components need improvement.

Acknowledgments

This research work was funded by CONICYT-PCHA/Doctorado_Nacional/año2013-folio21130634 and Fondecyt 1130621.

References

[1] COCHILCO, "Proyecciones del consumo de electricidad en la minería del cobre 2015-2016.," *COCHILCO, Comisión Chilena del Cobre. DE 21/2015*, 2015. [Online]. Available: https://www.cochilco.cl/ListadoTemtico/Proyeccion_del_consumo_de_electricidad_en_la_mineria_del_cobre_2015_-_2026_VF.pdf. [Accessed: 21-Sep-2016].
[2] COCHILCO, "Proyecciones del consumo de agua en la minería del cobre al 2026.," *COCHILCO, Comisión Chilena del Cobre. DEPP 16/2015*, 2015. [Online]. Available: https://www.cochilco.cl/ListadoTemtico/Proyeccion_de_consumo_de_agua_2015_al_2026.pdf#search=precio del agua en el norte. [Accessed: 21-Sep-2016].
[3] Ministerio-de-energia-Chile, "Balance nacional de energía 2015; 2017. [Online]. Available: http://dataset.cne.cl/Energia_Abierta/Reportes/Minenergia/ReporteBNE 2015.pdf. [Accessed: 21-Sep-2016].
[4] COCHILCO, "Informe de actualización del consumo energético de la minería del cobre al año 2015," *COCHILCO, Comisión Chilena del Cobre. DE 11/2016*; 2016. [Online]. Available: https://www.cochilco.cl/Mercado de Metales/Informe de Consumo de Energía 2015 RBA versión final.pdf. [accessed: 21-Sep-2016].
[5] Escobar RA, Cortés C, Pino A, Salgado M, Pereira EB, Martins FR, et al. Estimating the potential for solar energy utilization in Chile by satellite-derived data and ground station measurements. Sol Energy Nov. 2015;121:139–51.
[6] Al Moussawi H, Fardoun F, Louahlia-Gualous H. Review of tri-generation technologies: design evaluation, optimization, decision-making, and selection approach. Energy Convers Manage Jul. 2016;120:157–96.
[7] Dincer I, Rosen M. Exergy, environment and sustainable development. 2nd ed. Elsevier Science; 2012.
[8] IRENA. Renewable power generation costs in 2014: an overview; 2015.
[9] Al-Karaghouli A, Kazmerski LL. Energy consumption and water production cost of conventional and renewable-energy-powered desalination processes. Renew Sustain Energy Rev 2013;24:343–56.
[10] Sarbu I, Sebarchievici C. General review of solar-powered closed sorption refrigeration systems. Energy Convers Manage 2015;105:403–22.
[11] Modi A, Bühler F, Andreasen JG, Haglind F. A review of solar energy based heat and power generation systems. Renew Sustain Energy Rev 2017;67:1047–64.
[12] NREL, Aalborg CSP-Brønderslev CSP with ORC project, SolarPACES, 2017. [Online]. < https://www.nrel.gov/csp/solarpaces/project_detail.cfm/projectID=8316 > . [accessed: 06-Jul-2017].
[13] Moser M, Trieb F, Fichter T, Kern J. Renewable desalination: a methodology for cost comparison. Desalin Water Treat 2013;51(4–6):1171–89.
[14] Moser M, Trieb F, Fichter T, Kern J, Hess D. A flexible techno-economic model for the assessment of desalination plants driven by renewable energies. Desalin Water Treat 2014;3994(October):1–15.
[15] Fylaktos N, Mitra I, Tzamtzis G, Papanicolas CN. Economic analysis of an electricity and desalinated water cogeneration plant in Cyprus. Desalin Water Treat 2015;3994(September):1–18.
[16] Palenzuela P, Alarcón-Padilla D-C, Zaragoza G. Large-scale solar desalination by combination with CSP: Techno-economic analysis of different options for the Mediterranean Sea and the Arabian Gulf. Desalination 2015;366:130–8.
[17] Perdichizzi A, Barigozzi G, Franchini G, Ravelli S. Performance prediction of a CSP plant integrated with cooling production. Energy Proc 2015;75:436–43.
[18] Al-Sulaiman FA, Dincer I, Hamdullahpur F. Thermoeconomic optimization of three trigeneration systems using organic Rankine cycles: Part I – Formulations. Energy Convers Manage 2013;69(May):199–208.
[19] Al-Sulaiman FA, Dincer I, Hamdullahpur F. Thermoeconomic optimization of three trigeneration systems using organic Rankine cycles: Part II – Applications. Energy Convers Manage May 2013;69:209–16.
[20] Calise F, d'Accadia MD, Macaluso A, Piacentino A, Vanoli L. Exergetic and exergoeconomic analysis of a novel hybrid solar–geothermal polygeneration system producing energy and water. Energy Convers Manage 2016;115:200–20.
[21] Ortega-Delgado B, García-Rodríguez L, Alarcón-Padilla D-C. Thermoeconomic comparison of integrating seawater desalination processes in a concentrating solar power plant of 5 MWe. Desalination 2016;392:102–17.
[22] Wang J, Mao T. Cost allocation and sensitivity analysis of multi-products from biomass gasification combined cooling heating and power system based on the exergoeconomic methodology. Energy Convers Manage 2015;105:230–9.
[23] Escobar RA, Cortés C, Pino A, Pereira EB, Martins FR, Cardemil JM. Solar energy resource assessment in Chile: satellite estimation and ground station measurements. Renew Energy Nov. 2014;71:324–32.
[24] SimTech GmbH, IPSEpro Process Simulation Environment, Rev 5.0. SimTech Simulation Technology; 2011.
[25] Wagner MJ, Gilman P. Technical manual for the SAM physical trough model. Contract 2011;303(June):275–3000.
[26] NREL. System Advisor Model (SAM) Case Study: Andasol-1; 2013. p. 1–10.
[27] Bejan A, Tsatsaronis G, Moran M. Thermal design and optimization. 1st ed. John Wiley & Sons; 1996.
[28] Blanco-Marigorta AM, Victoria Sanchez-Henríquez M, Peña-Quintana JA. Exergetic comparison of two different cooling technologies for the power cycle of a thermal power plant. Energy Apr. 2011;36(4):1966–72.
[29] Montes MJ, Abánades A, Martínez-Val JM, Valdés M. Solar multiple optimization for a solar-only thermal power plant, using oil as heat transfer fluid in the parabolic trough collectors. Sol Energy Dec. 2009;83(12):2165–76.
[30] Zak G, Mitsos A, Hardt D. Master thesis. thermal desalination : structural optimization and integration in clean power and water. Massachusetts Institute of Technology; 2012.
[31] El-Dessouky HT, Ettouney HM. Fundamentals of salt water desalination. Elsevier; 2002.
[32] Palenzuela P, Hassan AS, Zaragoza G, Alarcón-Padilla D-C. Steady state model for multi-effect distillation case study: Plataforma Solar de Almería MED pilot plant. Desalination 2014;337(March):31–42.
[33] Herold K, Radermacher R, Klein S. Absorption chillers and heat pumps. 1st ed. CRC Press; 1996. [January 18, 1996].
[34] Petela R. Engineering thermodynamics of thermal radiation for solar power utilization. 1st ed. McGraw-Hill Education; 2010. [February 2, 2010].
[35] CNE. Informe de Proyección de precios de combustibles 2015-2030," CNE, Comisión Nacional de Energía, Chile., 2015. [Online]. Available: https://www.cne.cl/wp-content/uploads/2015/11/ResEx541_2015_Comb-informe-final-Informe-Proyecciones-Precios-Combustibles.pdf. [accessed: 21-Sep-2016].
[36] Mata-Torres C, Escobar RA, Cardemil JM, Simsek Y, Matute JA. Solar polygeneration for electricity production and desalination: case studies in Venezuela and northern Chile. Renew Energy 2017;101:387–98.
[37] Noro M, Lazzarin RM. Solar cooling between thermal and photovoltaic: an energy and economic comparative study in the Mediterranean conditions. Energy Aug. 2014;73:453–64.
[38] Turton R, Bailie R, Whiting W, Shaeiwitz J, Bhattacharyya D. Analysis synthesis, and design of chemical processes, 4th ed. Prentice Hall; 2012 [July 2, 2012].
[39] ELECDA. Tarifas actuales de suministro electrico," ELECDA, 2016. [Online]. < http://www.elecda.cl/wp-content/uploads/2016/10/Tarifas-de-Suministro_ELECDA_-Noviembre-2016.pdf > [accessed: 21-Nov-2016].
[40] Inodú, Utilización de bloques horarios en licitación de suministro a distribuidoras, 2014. Caso licitación SIC 2013/03-2o llamado, Inodú, 2014. [Online]. Available: http://www.acera.cl/wp-content/uploads/2015/02/Minuta-Acera-20122014b.pdf [accessed: 21-Sep-2016].
[41] Antofagasta A. Aguas Antofagasta, tarifas actuales, 2016. Aguas Antofagasta; 2016 [Online]. Available: http://www3.aguasantofagasta.cl/empresa/informacion-comercial/tarifas/tarifas-actuales.html [accessed: 21-Sep-2016].
[42] Ministerio de economía, "Ley 20257. Introduce modificaciones a la ley general de servicios eléctricos respecto de la generación de energía eléctrica con fuentes de energías renovables no convencionales; 2008. [Online]. Available: http://www.leychile.cl/Navegar/?idNorma=270212&idVersion=2008-04-01&idParte [accessed: 21-Sep-2016].
[43] SENDECO2. Precios del CO2, SENDECO2, 2016. [Online]. Available: http://www.sendeco2.com/es/precios-co2 [Accessed: 21-Nov-2016].